



RESEARCH ARTICLE

House dust mite-induced Akt-ERK1/2-C/EBP beta pathway triggers CCL20-mediated inflammation and epithelial-mesenchymal transition for airway remodeling

Shin-Young Park¹  | Min-Jeong Kang¹ | Nuri Jin¹ | So Young Lee² | Yun Young Lee³ | Sungsin Jo⁴ | Jeong Yun Eom⁵ | Heejae Han⁶ | Sook In Chung⁶ | Kiseok Jang⁵ | Tae-Hwan Kim⁴ | Jungwon Park⁶ | Joong-Soo Han¹ 

¹Biomedical Research Institute and Department of Biochemistry & Molecular Biology, College of Medicine, Hanyang University, Seoul, Republic of Korea

²EONE-DIAGNOMICS Genome Center Co. Ltd., Incheon, Republic of Korea

³Gencurix, Inc, Seoul, Republic of Korea

⁴Institute for Rheumatology Research, Hanyang University, Seoul, Republic of Korea

⁵Department of Pathology, Hanyang University Hospital, Seoul, Republic of Korea

⁶Institute for Allergy, Yonsei University College of Medicine, Seoul, Republic of Korea

Correspondence

Shin-Young Park and Joong-Soo Han, Biomedical Research Institute and Department of Biochemistry and Molecular Biology, College of Medicine, Hanyang University, 222 Wangsimni-ro, Seongdong-gu, Seoul 04763, Republic of Korea.

Email: ttokttoki@hanyang.ac.kr and jshah@hanyang.ac.kr

Funding information

National Research Foundation of Korea (NRF), Grant/Award Number: 2021R1A2C1008317 and 2018R1A1A1A05022185

Abstract

House dust mite (HDM) allergens cause inflammatory responses and chronic allergic diseases such as bronchial asthma and atopic dermatitis. Here, we investigate the mechanism by which HDM induces C-C chemokine ligand 20 (CCL20) expression to promote chronic inflammation and airway remodeling in an HDM-induced bronchial asthma mouse model. We showed that HDM increased CCL20 levels via the Akt-ERK1/2-C/EBP β pathway. To investigate the role of CCL20 in chronic airway inflammation and remodeling, we made a mouse model of CCL20-induced bronchial asthma. Treatment of anti-CCL20Ab in this mouse model showed the reduced airway hyper-responsiveness and inflammatory cell infiltration into peribronchial region by neutralizing CCL20. In addition, CCL20 induced the Nod-like receptor family, pyrin domain containing 3 (NLRP3) inflammasome activation through NLRP3 deubiquitination and transcriptional up-regulation in BEAS-2B cells. As expected, anti-CCL20Ab markedly suppressed NLRP3 activation induced by CCL20. Moreover, HDM-induced CCL20 leads to epithelial-mesenchymal transition in the lung epithelium which appears to be an important regulator of airway remodeling in allergic asthma. We also found

Abbreviations: AHR, airway hyper-responsiveness; BAL, Bronchoalveolar lavage; C/EBP β , CCAAT-enhancer-binding protein beta; CCL20, C-C chemokine ligand 20; EMT, epithelial to mesenchymal transition; H&E, hematoxylin and eosin; HDM, house dust mite; IL-1 β , interleukin-1 beta; NLRP3, Nod-like receptor family, pyrin domain-containing 3; p-AKT, phosphorylation of AKT; PAS, periodic acid-Schiff; p-ERK, phosphorylation of ERK1/2; TGF- β 1, transforming growth factor-beta 1; α -SMA, alpha-smooth muscle actin.

This is an open access article under the terms of the [Creative Commons Attribution](https://creativecommons.org/licenses/by/4.0/) License, which permits use, distribution and reproduction in any medium, provided the original work is properly cited.

© 2022 The Authors. *The FASEB Journal* published by Wiley Periodicals LLC on behalf of Federation of American Societies for Experimental Biology.

that anti-CCL20Ab attenuates airway inflammation and remodeling in an HDM-induced mouse model of bronchial asthma. Taken together, our results suggest that HDM-induced CCL20 is required for chronic inflammation that contributes airway remodeling in a mouse model of asthma.

KEYWORDS

airway remodeling, asthma, CCL20 (C-C chemokine ligand 20), house dust mites, NLRP3 (Nod-like receptor family pyrin domain containing 3)

1 | INTRODUCTION

House dust mite (HDM) is the most common allergen for allergic diseases such as atopic dermatitis, allergic rhinitis, and allergic asthma.¹ HDM allergens have been shown to induce an innate immune response, causing asthmatic airway inflammation.² Airway epithelial cells are the first physical barrier encountered by allergens. These cells are critical immune cells that play an important role in cytokine and chemokine production, which activate and recruit immune cells into the lungs.³ HDM extracts induce C-C chemokine ligand 20 (CCL20) secretion in airway epithelial cells, which recruits immature dendritic cells to the lung.⁴ CCL20 is a well-known chemokine that plays an important role in innate immunity.⁵ Moreover, CCL20 is upregulated in inflammatory diseases, such as allergic airway disease and rheumatoid arthritis.^{6–8} In addition, HDM-induced CCL20 secretion is related to oxidative stress and early allergic airway responses.³ However, the precise role of HDM-induced CCL20-mediated allergic airway inflammation remains to be elucidated.

Recent studies have drawn attention to the inflammasome machinery, particularly its activation, as an initiating factor in airway inflammation and pulmonary fibrosis.^{9,10} Inflammasomes are key components of the innate immune response to infection and cellular stress.¹¹ Among inflammasomes, the Nod-like receptor family, pyrin domain containing 3 (NLRP3)¹² is the most widely studied in relation to chronic airway inflammation. In addition, NLRP3 pharmacological inhibitors are being targeted for various diseases such as atherosclerosis, Alzheimer's diseases, and type II diabetes (T2D).¹³ Thus, NLRP3 inflammasome is an interesting molecule as a potential therapeutic target. NLRP3 inflammasome activation requires sequential priming and activation. The NLRP3 priming step can be divided into two parts: nuclear factor (NF)- κ B-dependent transcriptional NLRP3 upregulation and post-translational NLRP3 modification (non-transcriptional).¹⁴ NLRP3 activation initiates NLRP3 inflammasome complex assembly, resulting in the maturation of caspase-1, a cysteine protease that converts inactive pro-interleukin (IL)-1 β to active inflammatory IL-1 β .¹⁵

Recent studies have reported that NLRP3-induced IL-1 β activation contributes to lung fibrosis, including airway inflammation and remodeling.^{9,10,16} Some studies have shown that CCL20 activation is closely related to IL-1 β -mediated pro-inflammatory responses and diseases.^{17,18} In addition, chemokines including CCL20 have been identified as a subgroup in the molecular network of NLRP3 inflammasome activation-responsive genes.¹⁹ However, the molecular mechanism regulating NLRP3 activation by CCL20 remains largely unknown.

Airway remodeling is a result of increased fibroblast dysfunction. Fibroblasts are located in the interstitial spaces surrounding the airways. In the damage around the airway due to inflammation, fibroblast is transformed into myofibroblast and eventually becomes fibrosis. Epithelial-mesenchymal transition (EMT) has been implicated in wound healing, fibrosis, and cancer metastasis.²⁰ When fibroblasts become activated, they are differentiated into α -smooth muscle actin (α -SMA) expressing myofibroblasts. EMT is accompanied by molecular change by various signaling pathways which promote the repression of E-cadherin expression through the activation of fibronectin and vimentin in the loss of epithelial features.^{21,22} It has been known that inflammatory factors such as IL-1 β and chronic transforming growth factor (TGF)- β 1 are mainly involved in bronchial epithelium damage, mucus production, and subepithelial fibrosis,²³ but its function in HDM-mediated airway inflammation and EMT production has not yet been investigated. In addition, CCL20-related EMT has been mostly studied in cancer, and its role in airway remodeling remains to be elucidated.

In the present study, we investigated the potential role of HDM-induced CCL20 in allergic airway remodeling and chronic inflammation in bronchial asthma using experimental asthma mouse models and human bronchial epithelial cell lines. Our results clearly show that HDM-induced CCL20 is regulated by the Akt-ERK1/2-C/EBP β pathway, which enhances NLRP3 inflammasome activation. Furthermore, we demonstrated that CCL20-mediated NLRP3 activation is required for profibrotic factors and EMT progression in asthmatic airway remodeling. To the best of knowledge, this is the first report to

elucidate the mechanism for CCL20 induction by HDM leading to activation of inflammasome and EMT production. Thus, our results suggest that CCL20 may be a novel therapeutic target for the regulation of airway inflammation and remodeling in allergic asthma.

2 | MATERIALS AND METHODS

2.1 | Generation of the HDM-induced asthma model

Eight-week-old female BALB/c mice were purchased from Orient Bio (Daejeon, Korea). Mice were sensitized by intranasal administration of HDM (30 µg/mouse) or saline (Sham) total seven times for 17 days. For the CCL20 neutralizing study, mice were sensitized by intranasal administration of CCL20 (0.25 µg/mouse) or saline (Sham) 5 times per week for 4 weeks. For the HMD-mediated CCL20 neutralizing study, mice were sensitized by intranasal administration of HDM (30 µg/mouse) or saline (Sham) 3 times per week for 4 weeks. Mice were treated intranasally with anti-CCL20Ab (2.5 µg/mouse) every time when CCL20 was administered. The mice were sacrificed, and the protein delivery efficiency and pathological changes in the lungs were analyzed. All experimental animal procedures were approved by the Institutional Animal Care and Use Committee (IACUC) at Hanyang College of Medicine (approval number 2019-0052).

2.2 | Cell culture

Human airway epithelial cells transformed with adenovirus 12-SV40 virus hybrid (BEAS-2B cells) were purchased from the American Type Culture Collection. BEAS-2B cells were cultured in Dulbecco's modified Eagle's medium (DMEM)/F12 with 10% fetal bovine serum, 100 U/mL penicillin, and 100 ng/ml streptomycin (Invitrogen, Carlsbad, CA, USA) at 37°C in humidified air with 5% CO₂. Human diploid lung IMR90 fibroblasts were cultured in minimum essential medium (Welgene, Daejeon, Korea) supplemented with 10% fetal bovine serum at 37°C in humidified air with 5% CO₂.

2.3 | RNA extraction and reverse transcription-quantitative polymerase chain reaction

Total RNA was extracted from cultured cells using RNeasy Plus (Takara Bio Inc., Ohtsu, Japan). For quantitative real-time PCR, 300 ng of purified total RNA was used for reverse

transcription using GoScript reverse transcriptase and random primers (Promega Corporation, Madison, WI, USA). Real-time PCR was performed using a SensiFAST SYBR No-ROX Kit (Bioline, London, UK) on a CFX Connect Real-Time PCR Detection System (Bio-Rad). The primers used for reverse transcription-quantitative polymerase chain reaction are listed in Table S1. Thermocycling conditions were 95°C for 10 min, followed by 40 cycles at 95°C for 15 s and 60°C for 1 min. Each sample was tested in duplicate, and at least three biological replicates were examined. Relative quantification was performed using the $2^{-\Delta\Delta Ct}$ method. Relative gene expression was normalized to that of the internal control glyceraldehyde 3-phosphate dehydrogenase.

2.4 | Western blot assays

Cells were lysed in an ice-cold hypotonic lysis buffer (10 mM Tris-HCl [pH 7.5], 10 mM NaCl, 10 mM EDTA, 0.5% Triton X-100 containing, complete EDTA-free protease inhibitor cocktail; Roche Diagnostics, Indianapolis, IN, USA). Protein samples (15–30 µg) were loaded onto a NEXT GEL® 7.5% or 15% gel (Amresco, Solon, OH, USA) and transferred to poly(vinylidene fluoride) membranes (Merck Millipore) after electrophoresis. After blocking with 5% non-fat-dried milk for 1 h, membranes were incubated with primary antibodies followed by horseradish peroxidase (HRP)-conjugated secondary antibody (anti-mouse IgG (#7076) and anti-rabbit IgG (#7074), 1:2000) (New England Biolabs, Beverly, MA, USA). Specific bands were detected using an ECL substrate (Thermo Fisher Scientific) and quantified using Quantity Ones® software (Bio Rad).

2.5 | Transient cell transfection

pBabe-puro and pBabe-C/EBPβ plasmids were obtained from Addgene (Cambridge, MA, USA). Then, 5 µg vector control or C/EBPβ was transiently transfected into BEAS-2B cells using Lipofectamine 2000 reagent (Invitrogen) for 48 h. After transfection, the cells were serum-starved for 18 h and then treated with HDM. For C/EBPβ silencing experiments, C/EBPβ siRNA (sense: 5'-acaacaucgccgugcgcauu-3', antisense: 5'-uugcgacggcgauuguuuu-3') and negative control siRNA (sense: 5'-ccucgugccguuccaucagguuu-3', antisense: 5'-cuaccugauggaacggcagagguu-3') were purchased from Genolution (Seoul, Korea). Dectin-1 siRNA (#sc-63276) was purchased from Santa Cruz Biotechnology. RELA siRNA (ON-TARGET plus SMARTpool #L-003533-00-00005) and NLRP3 siRNA (ON-TARGET plus SMARTpool #L-017367-00-00005) were purchased from Dharmacon (Lafayette, CO, USA). All siRNAs were introduced into BEAS-2B or IMR90

cells using Lipofectamine RNAiMAX transfection reagent (Invitrogen).

2.6 | Immunofluorescence staining

Cells were fixed with 4% (w/v) paraformaldehyde in phosphate-buffered saline (PBS) for 20 min and washed three times with 0.1% BSA in PBS. The cells were then blocked with 10% normal goat serum, 0.3% Triton X-100, and 0.1% BSA in PBS for 1 h. Next, the cells were immunostained with rabbit polyclonal anti-CCL20/MIP-3 α (#bs-1268R, 1:200), mouse monoclonal anti-E-cadherin (#33-4000, 1:400), mouse monoclonal anti-F-actin (#ab130935, 1:500), and mouse monoclonal anti- α -SMA (#MAB1420, 1:100) primary antibodies at 4°C overnight. The cells were then washed three times with PBS and then incubated with fluorescence-conjugated secondary antibodies (Alexa Fluor® 488 [#A11011, #A11008] and 594 [#A11005], 1:2000; Life Technologies, Eugene, OR, USA) for 1 h. Finally, the cells were washed three times with PBS and mounted with Vectashield (Vector Laboratories, Burlingame, CA, USA) containing 4, 6-diamidino-2-phenylindole mounting medium. Immunoreactive cells were analyzed using an epifluorescence microscope (Nikon Instruments, Melville, NY, USA) at magnifications of 20–40 \times .

2.7 | Enzyme-linked immunosorbent assay

Cell supernatants were collected and tested for CCL20 using human CCL20/MIP-3 α Immunoassay (#DA3A00, R&D Systems). For the mouse model experiments, CCL20 was detected using mouse CCL20/MIP-3 α DuoSet® enzyme-linked immunosorbent assay (ELISA) kit (#DY760, R&D Systems). Plates were read on a SpectraMax M2 microplate reader (Molecular Devices, Sunnyvale, CA, USA) and analyzed using SOFTmax analysis software (Molecular Devices).

2.8 | Lung lysate analysis

Lung tissues were homogenized in 20 ml/g tissue protein extraction reagent (Thermo Fisher Scientific) using a tissue homogenizer (Biospec Products, Bartlesville, OK, USA). Homogenates were incubated at 4°C for 30 min and then centrifuged at 1000 \times g for 10 min. The supernatants were collected, passed through a 0.45-micron filter (Gelman Sciences, Ann Arbor, MI, USA), and stored at –70°C until the assessment of cytokine levels.

2.9 | Immunohistochemistry

Lung tissues were prepared as paraffin blocks and sectioned to 3- μ m thickness. The sections were then deparaffinized in xylene. After xylene was removed with absolute ethanol, the slides were treated with 3% H₂O₂ to block endogenous peroxidase activity. Slides were incubated with the following primary antibodies: CCL20/MIP-3 α (#bs-1268R, 1:200), IL-1 β (#12242S, 1:150), NLRP3 (#ABF23, 1:100), α -SMA (#MAB1420, 1:200), and TGF- β 1 (#sc-130348, 1:150). The secondary antibody was biotinylated goat anti-rabbit or anti-mouse antibody at 1:200 dilution and signals were visualized using a mouse and rabbit-specific HRP/DAB detection IHC kit (#ab64264, Abcam). For histological analysis, slides with attached sections were stained with periodic acid-Schiff or Masson's trichrome stain. The degree of proliferation of goblet cells was compared by counting the number of periodic acid-Schiff (PAS)-positive cells in 100 μ m of the perimeter of the basement membrane. The number of goblet cells was counted from three bronchi that were similar in size and had a circular shape based on the length of the perimeter of the basement membrane, and the average number of goblet cells per 100 μ m of the perimeter of the basement membrane was calculated. The area of peribronchial trichrome staining in the mouse lung is expressed as the area of trichrome staining per μ m length of the basement membrane of bronchioles. At least, 10 bronchioles with internal diameters of 150–200 μ m in each slide were counted. For semi-quantitative analysis of the protein expression of CCL20, α -SMA, or TGF- β , the sections are measured using a quantitative digital image analysis system (Zeiss Zen lite image analysis software [blue edition], Carl Zeiss Microimaging, Göttingen, Germany). Images were evaluated using a Zeiss Cell Observer (Zeiss Axiovision 4.6 software).

2.10 | Airway hyper-responsiveness analysis

Mice were anesthetized (pentobarbital sodium, intraperitoneally), ventilated with a flexiVent 5.1 ventilator (SCIREQ, Montreal, Canada), and challenged with saline aerosol followed by increasing concentrations of methacholine (MeCh; Sigma-Aldrich, St. Louis, MO, USA). Aerosols were generated with an ultrasonic nebulizer (Omron Healthcare, Kyoto, Japan) and delivered through the flexiVent inspiratory line of the flexiVent using a bias flow of medical air. Measurements were made twice at 1 min intervals following each delivery of MeCh aerosol.

2.11 | Bronchoalveolar lavage fluid analysis

The lungs were lavaged with 1 ml Hank's balanced salt solution via a tracheostomy tube. Total cell numbers were counted using a hemocytometer. After lavage, the Bronchoalveolar lavage (BAL) fluid was centrifuged, and BAL cell smears were prepared by cytocentrifugation (Cytospin3, Thermo Fisher Scientific, Waltham, MA, USA) at 1000 rpm for 3 min. BAL cells were stained with hemacolor staining kits (Merck Millipore, Billerica, MA, USA) and classified as neutrophils, eosinophils, lymphocytes, or macrophages. The cells were differentially counted until the total counted number reached at least 200, using standard hemocytologic procedures.

2.12 | RNA-sequencing of mouse lung tissue

Total RNA was isolated from mouse lung tissue using RNAiso Plus (Takara Bio Inc.). RNA quality was assessed by Agilent 2100 bioanalyzer using the RNA 6000 Nano Chip (Agilent Technologies, Amstelveen, The Netherlands), and RNA quantification was performed using ND-2000 Spectrophotometer (Thermo Inc., DE, USA). For each samples, the construction of library was performed using QuanSeq 3' mRNA-Seq Library Prep Kit (Lexogen, Inc., Austria) according to the manufacturer's instructions. High-throughput sequencing was performed as single-end 75 sequencing using NextSeq 500 (Illumina, Inc., USA).

2.13 | RNA-seq data analysis

QuantSeq 3' mRNA-Seq reads were aligned using Bowtie2. DEGs were determined based on counts from unique and multiple alignments using coverage in Bedtools. Data mining and graphic visualization were performed using ExDEGA (Ebiogen Inc., Seoul, Korea). Go analysis was performed using DAVID (<http://david.abcc.ncifcrf.gov/>) with default parameters, and enrichment plots were generated using gene set enrichment analysis (GSEA). Hierarchical Clustering Heatmap was analyzed using ExDEGA GraphicPlus (Ebiogen Inc.).

2.14 | Statistical analysis

All quantitative data were expressed as the mean \pm SEM. Binary comparisons were made using Student *t* test. Multiple group comparisons were made using One-way ANOVA,

with post hoc comparison via Tukey's test, or Bonferroni's post hoc test, as appropriate. RNA-seq data, two-sample *t* test with unequal variance was applied. All analyses were performed using SPSS 17.0 software (SPSS Inc., Chicago, IL, USA). Statistical significance was set at $p < .05$.

3 | RESULTS

3.1 | HDM induces CCL20 expression through the dectin-1 receptor

To determine whether HDM induce CCL20 expression, BEAS-2B cells were stimulated with HDM. As shown in Figure 1A,B, the CCL20 levels were increased by HDM treatment when compared with controls. HDM induced CCL20 gene expression within 30 min after exposure, which indicates that HDM triggers CCL20 transcription directly. Immunofluorescence analysis of BEAS-2B cells revealed that we found that CCL20 cytosolic concentration was enhanced by HDM stimulation for 6 h (Figure 1C). Furthermore, we showed that CCL20 protein levels in the BEAS-2B cell supernatants were significantly increased by HDM treatment ($p < .05$), and peaked at 24 h (Figure 1D). CCL20 secretion could be mediated by the binding of HDM-derived β -glucans to C-type lectin receptors, also called dectins.²⁴ Among them, dectin-1 plays an essential role in innate immune responses in airway epithelial cells.²⁵ To determine whether the dectin-1 receptor is related to HDM-induced CCL20 production, BEAS-2B cells were transfected with dectin-1 siRNA or control siRNA. Dectin-1 knock-down efficiently reduced HDM-induced CCL20 expression, suggesting that the dectin-1 receptor is critical for HDM-mediated CCL20 production (Figure 1E,F). To confirm whether the in vitro experimental results could be reproduced in an in vivo animal model, we examined HDM-induced airway inflammation in a mouse model (Figure 1G). Histological examination of CCL20 staining showed that intranasal challenge with HDM increased CCL20 expression (Figure 1H). Consistently, HDM intranasal administration increased CCL20 mRNA levels and protein levels (Figure 1I–K). In addition, hematoxylin and eosin (H&E) and PAS staining showed that HDM induced airway thickening and increased the number of mucus-containing goblet cells around the bronchial airway (Figure 1L,M). We also measured the fibrotic area based on Masson's trichrome staining, which showed that HDM-treated mice exhibited high peribronchial fibrosis in the lung (Figure 1N). These results suggest that HDM-induced CCL20 plays a role in bronchial airway remodeling. Therefore, we further examined the role of HDM-induced CCL20 in asthmatic airway remodeling.

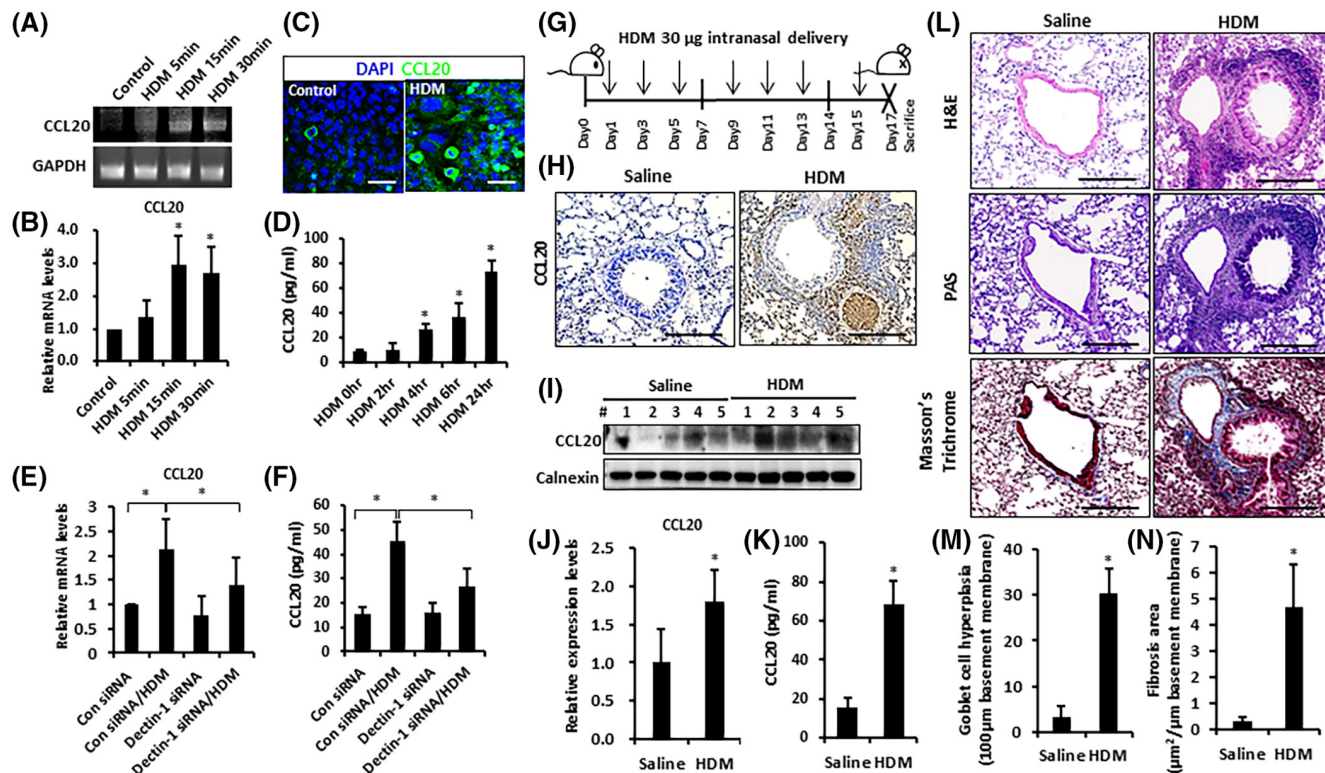


FIGURE 1 House dust mite (HDM) increases C-C chemokine ligand 20 (CCL20) expression in human bronchial epithelial cells. (A and B) BEAS-2B cells were treated with HDM (10 $\mu\text{g}/\text{ml}$) for the indicated time. The cells were harvested, and total RNA was isolated using TRIzol reagent. CCL20 transcripts were analyzed by reverse transcription-quantitative polymerase chain reaction (RT-qPCR). Data represent the mean \pm standard error of the mean (SEM) of three independent experiments. $*p < .05$; one-way analysis of variance (ANOVA). (C) The cells were treated with HDM (10 $\mu\text{g}/\text{ml}$) for 6 h and stained with anti-CCL20 (green) antibody. CCL20-positive cells were counted in randomly selected areas from at least three cultures. (D) The cells in 96-well culture plates were treated with HDM (10 $\mu\text{g}/\text{ml}$) for the indicated times. CCL20 levels were measured using enzyme-linked immunosorbent assay (ELISA). Data represent the mean \pm SEM of three independent experiments. $*p < .05$; one-way ANOVA. (E) BEAS-2B cells were transfected with 100 nM dectin-1 siRNA or control siRNA for 72 h and then treated with HDM (10 $\mu\text{g}/\text{ml}$) for 30 min. The cells were harvested, and total RNA was isolated using TRIzol reagent. CCL20 transcripts were analyzed by RT-qPCR. Data represent the mean \pm SEM of three independent experiments. $*p < .05$; one-way ANOVA. (F) The cells in 96-well culture plates were transfected with 100 nM dectin-1 siRNAs or control siRNA for 72 h and then treated with HDM (10 $\mu\text{g}/\text{ml}$) for 24 h. CCL20 levels were measured by ELISA. Data represent the mean \pm SEM of three independent experiments. $*p < .05$; one-way ANOVA. (G) Schedule for preparation of the allergic airway inflammation model. Eight-week-old BALB/c mice were intranasally administered 30 μg of HDM on days 1, 3, 5, 9, 11, 13 and 15. Sacrifice was performed on the 17th day. (H) Tissue sections were stained using anti-CCL20. (I and J) Expression of mRNA and protein isolated from lung lysates was analyzed by RT-qPCR and western blotting, respectively. Data represent the mean \pm SEM ($n = 5$ for each group). $*p < .05$; Student t test. (K) CCL20 was measured in lung homogenates by ELISA. Data represent the mean \pm SEM ($n = 5$ for each group). $*p < .05$; Student t test. (L) Tissue sections were stained using hematoxylin and eosin (H&E), periodic acid-Schiff (PAS), and Masson's Trichrome. (M and N) The number of goblet cells and the fibrotic area were analyzed using Zeiss Cell Observer. Data are expressed as the mean \pm SEM ($n = 5$ for each group). $*p < .05$; Student t test.

3.2 | HDM-induced CCL20 expression is regulated by the Akt-ERK1/2-C/EBP β pathway

A recent study has demonstrated that C/EBP β is a critical regulator of CCL20 gene expression in normal human keratinocytes, and it activates the CCL20 promoter via two proximal binding sites.²⁶ The transcription factor C/EBP β plays an important role in cellular responses to inflammatory stimuli and general responses to pathogens in several cell types.^{27,28} Thus, the effect of C/EBP β on CCL20 gene

expression was examined in BEAS-2B cells after HDM exposure. C/EBP β overexpression resulted in increased CCL20 gene expression when compared to vector transfected control cells treated with HDM (Figure 2A,B), whereas C/EBP β knockdown attenuated CCL20 gene expression when compared to control siRNA transfected cells treated with HDM (Figure 2C,D). These results show that C/EBP β is required for HDM-induced CCL20 gene expression.

As other studies have shown that ERK1/2 activates C/EBP β -dependent gene expression,²⁹ we examined the

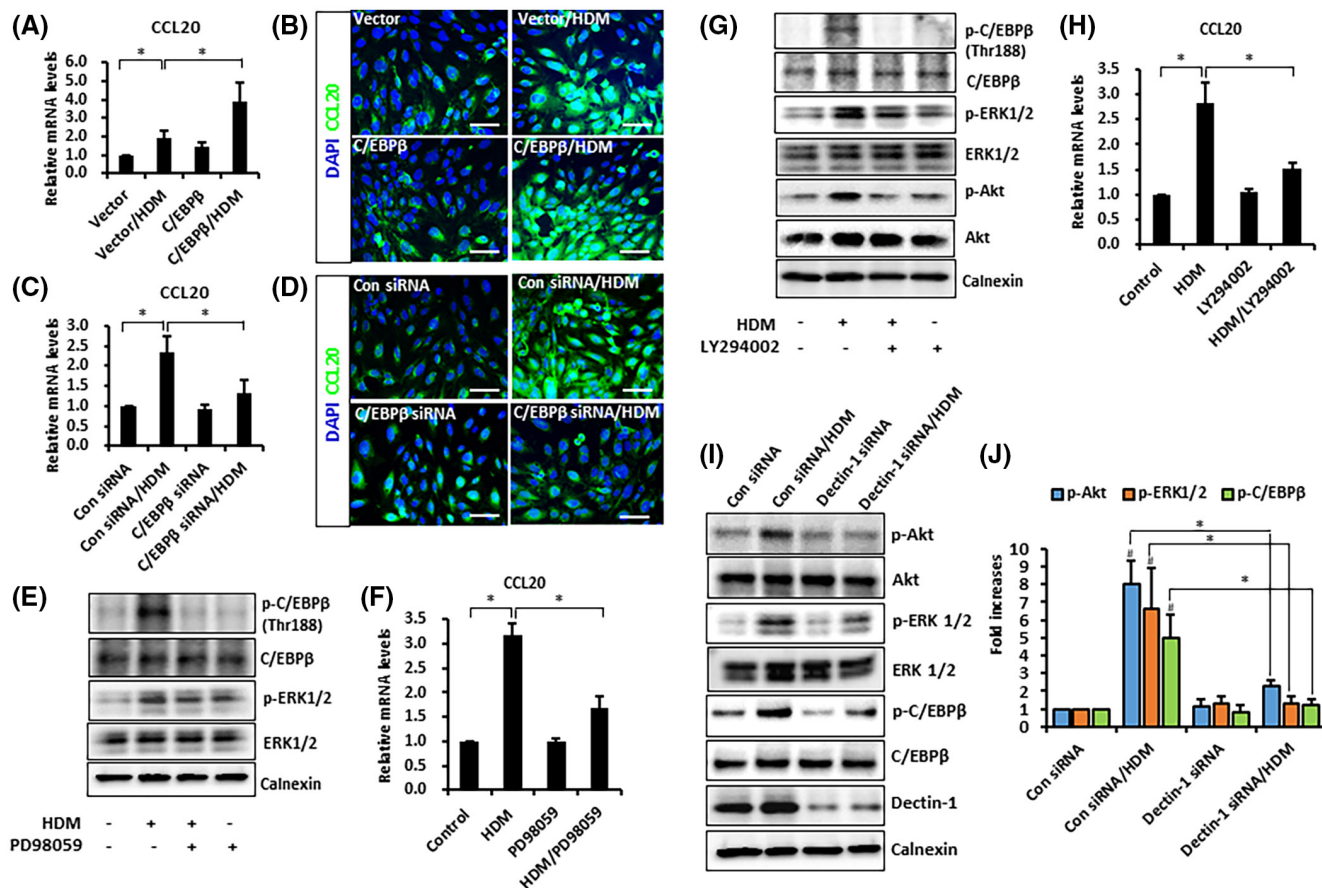


FIGURE 2 House dust mite (HDM) activates the Akt-ERK1/2-C/EBP β pathway in BEAS-2B cells. (A and B) BEAS-2B cells were transfected with vector or C/EBP β plasmid for 48 h, and then treated with HDM (10 μ g/ml) for (A) 30 min and (B) 6 h. The cells were harvested, and total RNA was isolated using TRIzol reagent. Data represent the mean \pm standard error of the mean (SEM) of three independent experiments. * p < .05; one-way analysis of variance (ANOVA). (A) C-C chemokine ligand 20 (CCL20) transcripts were analyzed by reverse transcription-quantitative polymerase chain reaction (RT-qPCR). (B) The cells were stained with anti-CCL20 (green) antibody. (C and D) The cells were transfected with control siRNA or C/EBP β siRNA for 48 h, and then treated with HDM (10 μ g/ml) for (C) 30 min and (D) 6 h. (C) The cells were harvested, and total RNA was isolated using TRIzol reagent. CCL20 transcripts were analyzed by RT-qPCR. Data represent the mean \pm SEM of three independent experiments. * p < .05; one-way ANOVA. (D) The cells were stained with anti-CCL20 (green) antibody. (E and F) The cells were pretreated with 2 μ M PD98059, an ERK1/2 inhibitor, for 1 h and treated with HDM (10 μ g/ml) for (E) 15 or (F) 30 min. (E) Protein expression was analyzed using western blotting and (F) CCL20 transcript levels were analyzed using RT-qPCR. Data represent the mean \pm SEM of three independent experiments. * p < .05; one-way ANOVA. (G and H) The cells were pretreated with 1 μ M LY294002, an AKT inhibitor, for 1 h and stimulated with HDM (10 μ g/ml) for (G) 15 or (H) 30 min. (G) Protein levels were analyzed using western blotting and (H) CCL20 transcript levels were analyzed using RT-qPCR. Data represent the mean \pm SEM of three independent experiments. * p < .05; one-way ANOVA. (I and J) The cells were transfected with 100 nM dectin-1 siRNA or control siRNA for 72 h and then stimulated with HDM (10 μ g/ml) for 15 min. Protein levels were analyzed using western blotting. Data represent the mean \pm SEM of three independent experiments. * p < .05; * p < .05, con siRNA; one-way ANOVA.

effect of ERK1/2 on C/EBP β -dependent CCL20 expression. Cells were treated with HDM in the presence or the absence of PD98059 specific ERK1/2 inhibitor, and C/EBP β activation and CCL20 gene expression were determined. Our results indicated that PD98059 strongly blocked C/EBP β activation and subsequent HDM-induced CCL20 gene expression (Figure 2E,F). Moreover, Akt has been shown to promote C/EBP β activation. When the cells were pretreated with LY294002, a specific PI3K/Akt inhibitor, HDM-induced C/EBP β activation was

completely blocked (Figure 2G). Furthermore, when the activity of Akt was blocked, remarkable inhibition of ERK1/2 activation and CCL20 expression was observed (Figure 2G,H). Next, we investigated whether the dectin-1 receptor is involved in the HDM-induced Akt-ERK1/2-C/EBP β pathway. We showed that dectin-1 knockdown suppressed HDM-induced Akt-ERK1/2-C/EBP β activation (Figure 2I,J), suggesting that the dectin-1-associated Akt-ERK1/2-C/EBP β pathway is crucial for HDM-induced CCL20 expression.

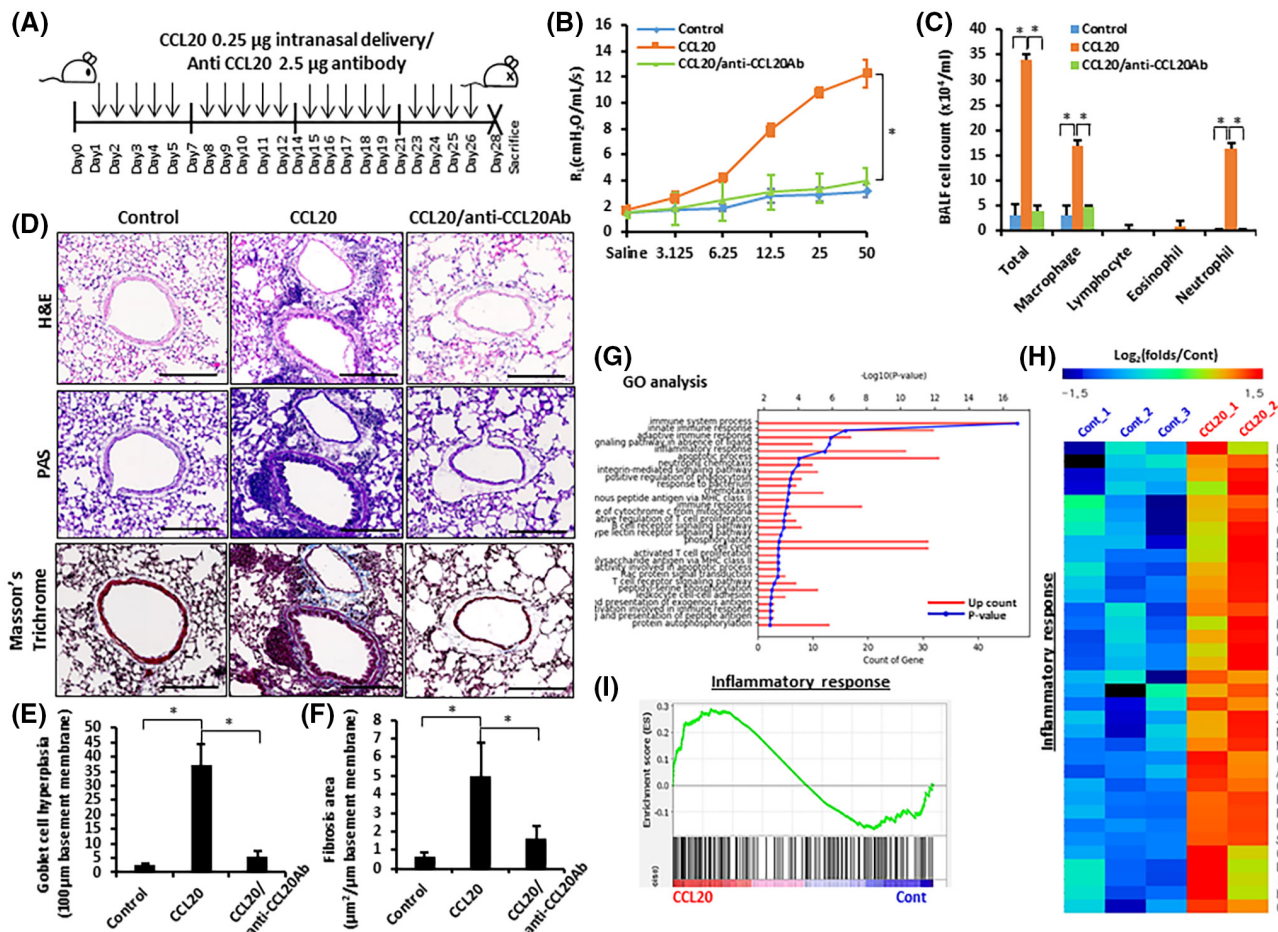


FIGURE 3 C-C chemokine ligand 20 (CCL20) regulates airway hyper-responsiveness and airway remodeling in a mouse model of bronchial asthma. (A) Schedule for preparation of the allergic airway inflammation model. Eight-week-old BALB/c mice were intranasally administered CCL20 (0.25 µg) or co-treated with CCL20 (0.25 µg) and anti-CCL20Ab (2.5 µg) for 5 days/week for 4 weeks. Sacrifice was performed on the 28th day. (B) Airway hyper-responsiveness (AHR) was measured using airway resistance and compliance to metacholine. Data represent the mean \pm standard error of the mean (SEM) ($n = 5$ for each group). $*p < .05$; one-way analysis of variance (ANOVA). (C) Immune cells in BAL fluid were counted. Data represent the mean \pm SEM ($n = 5$ for each group). $*p < .05$; one-way ANOVA. (D) Tissue sections were stained using hematoxylin and eosin (H&E), periodic acid-Schiff (PAS) and Masson's Trichrome and observed by brightfield microscopy. The number of goblet cells (E) and the fibrotic area (F) were analyzed using Zeiss Cell Observer. Data are expressed as the mean \pm SEM ($n = 5$ for each group). $*p < .05$; one-way ANOVA. (G) Gene ontology (GO) analyses for the genes upregulated in CCL20-treated mice compared with control mice. Red lines indicate the number of genes under the designated Go term pathway. Blue lines with dot indicate p values. (H) Heatmap showing fold changes of the selected genes from inflammatory response in CCL20-treated mice (CCL20_1 and CCL20_2) compared with control mice (Cont_1, Cont_2, and Cont_3). (I) GSEA for inflammatory response genes sets enriched in CCL20-treated mice (CCL20) versus Control mice (Cont).

3.3 | CCL20 regulates airway hyper-responsiveness and remodeling of airway in a mouse model of bronchial asthma

To investigate whether CCL20 plays a role in bronchial airway remodeling, we developed a mouse model of CCL20-induced airway inflammation, as described in Figure 3A. In these experiments, Saline (control), 0.25 µg CCL20, or 0.25 µg CCL20 with 2.5 µg of neutralizing anti-CCL20 antibody (anti-CCL20Ab) was intranasally administered (Figure 3A). On day 28, the mice were anesthetized, and airway resistance to MeCh was measured using a

flexiVent system (Figure 3B). CCL20-induced airway hyper-responsiveness (AHR) to MeCh was significantly attenuated by anti-CCL20Ab compared to CCL20-treated mice ($p < .05$), suggesting that anti-CCL20Ab strongly suppresses allergic inflammation and AHR. Consistent with the AHR observation, the number of inflammatory cells, especially macrophages and neutrophils, was significantly decreased in the anti-CCL20Ab co-treated mice compared to CCL20-treated mice (Figure 3C). Histological analysis of lung tissue from these mice demonstrated significant inflammation and epithelial damage when treated with CCL20 (Figure 3D). PAS staining showed a marked

reduction in the total inflammatory cell number around the airway, blood vessels, and goblet cells in the anti-CCL20Ab-co-treated mice compared to CCL20-treated mice (Figure 3D,E). In addition, Masson's trichrome staining revealed dense collagen deposition/subepithelial fibrosis surrounding the airways and vessels of lung tissues in the CCL20-treated mice compared to the control group (Figure 3D,F). In contrast, co-treatment of anti-CCL20Ab obviously reduced peribronchial fibrosis that observed in CCL20-treated mice. Thus, we can conclude that CCL20 regulates AHR and bronchial airway remodeling.

To investigate the molecular mechanism underlying the CCL20-mediated bronchial airway remodeling, RNA-seq was performed. We identified upregulated 623 genes between control and CCL20-treated mice with >1.5-fold differences in expression and p -value <.05 (Supporting Information 1). Among these, 109 genes were enriched in the gene ontologies associated with immune and inflammatory process (Figure 3G, Supporting Information 2). Next, we looked into the detailed inflammatory categories of the differentially expressed genes (DEGs) using the hierarchical clustering analysis (Figure 3H). Moreover, GSEA result confirmed the significant up-regulation of genes involved in inflammatory response in CCL20-treated mice compared with control mice (Figure 3I). These RNA-seq data suggest that bronchial airway remodeling by CCL20 is closely related to the inflammatory process.

3.4 | CCL20 participates in NLRP3 inflammasome activation

Inflammasome is emerging as a key factor in inflammation and the innate immune system. Interestingly, our RNA-seq data also showed that inflammasome-related genes, such as NLRP3 (fold change = 1.511 and p -value = .018) and IL-1 β (fold change = 3.566 and p -value = .003), were significantly increased in CCL20-treated mice (Figure 4A). Furthermore, we confirmed the expression of *NLRPs* in BEAS-2B cells. As shown in Figure S1, among the *NLRPs*, the expression of *NLRP3* was remarkably increased by CCL20 treatment, and it was significantly decreased by anti-CCL20Ab treatment. NLRP3 is the most extensively studied inflammasome in inflammatory airway diseases such as asthma.^{30,31} Previous studies have reported that NLRP3 is involved in inflammatory cell activation, particularly neutrophils and macrophages.^{32,33} Interestingly, our study also showed that the number of macrophages and neutrophils was significantly increased in CCL20-treated mice compared to control mice (Figure 3C). Therefore, we determined whether NLRP3 activation is related to CCL20-induced airway inflammation. The NLRP3 inflammasome triggers caspase-1 activation, which then

induces IL-1 β secretion. As shown in Figure 4B,C, CCL20 induced NLRP3 inflammasome activation, including caspase-1 activation and IL-1 β secretion, which were decreased by anti-CCL20Ab treatment of mouse models. We also showed that CCL20-induced NLRP3, caspase-1, and IL-1 β levels were decreased by anti-CCL20Ab treatment of BEAS-2B cells (Figure 4D–F). Furthermore, we confirmed that CCL20-induced NLRP3 activation mediated caspase-1 and IL-1 β activation using NLRP3 siRNA (Figure 4G–I). These results indicate that CCL20 participates in NLRP3 inflammasome activation during airway inflammation.

NLRP3 inflammasome activation controls one or several of the following events: (1) early or intermediate post-translational NLRP3 modifications, such as ubiquitination, which switches the NLRP3 to a form competent for further activation or (2) late transcriptional upregulation of NLRP3, inflammasome substrates including pro-IL-1 β , and probably other key regulator(s).¹⁴ Thus, we investigated which of these processes are controlled by CCL20-mediated NLRP3 activation. First, we examined whether CCL20 affects NLRP3 ubiquitination. As shown in Figure 4J, NLRP3 ubiquitination was diminished by CCL20 treatment, and was reversed by anti-CCL20Ab treatment (Figure 4K). These results indicate that CCL20 promoted NLRP3 deubiquitination. Since transcriptional regulation of NLRP3 is regulated by NF- κ B,¹⁹ we examined whether NF- κ B activation mediates CCL20-stimulated NLRP3 transcriptional upregulation. When BEAS-2B cells were transfected with NF- κ B siRNA, CCL20-induced NLRP3 expression decreased compared to control siRNA with CCL20 (Figure 4L,M). Taken together, these data indicate that CCL20-mediated NLRP3 activation is caused by two processes: (1) inhibition of NLRP3 ubiquitination and (2) NF- κ B-dependent transcriptional upregulation.

3.5 | CCL20 promotes EMT in human bronchial epithelial cells

Loss of epithelial integrity plays a key role in the development of airway remodeling.³⁴ The airway epithelium forms the first barrier against deposited aeroallergens. The barrier function is maintained by intracellular contact through homophilic E-cadherin interactions. Reduced E-cadherin-mediated cell–cell contacts are an important component of EMT, which is central to long-term structural changes within the airways.³⁵ HDM promotes EMT in the human bronchial epithelium.³⁶ We observed that exposure of mice to HDM increased the expression of the mesenchymal marker vimentin and decreased E-cadherin expression (Figure S2A–C). We also showed that treatment of BEAS-2B cells with HDM resulted in a time-dependent increase in vimentin expression and decrease

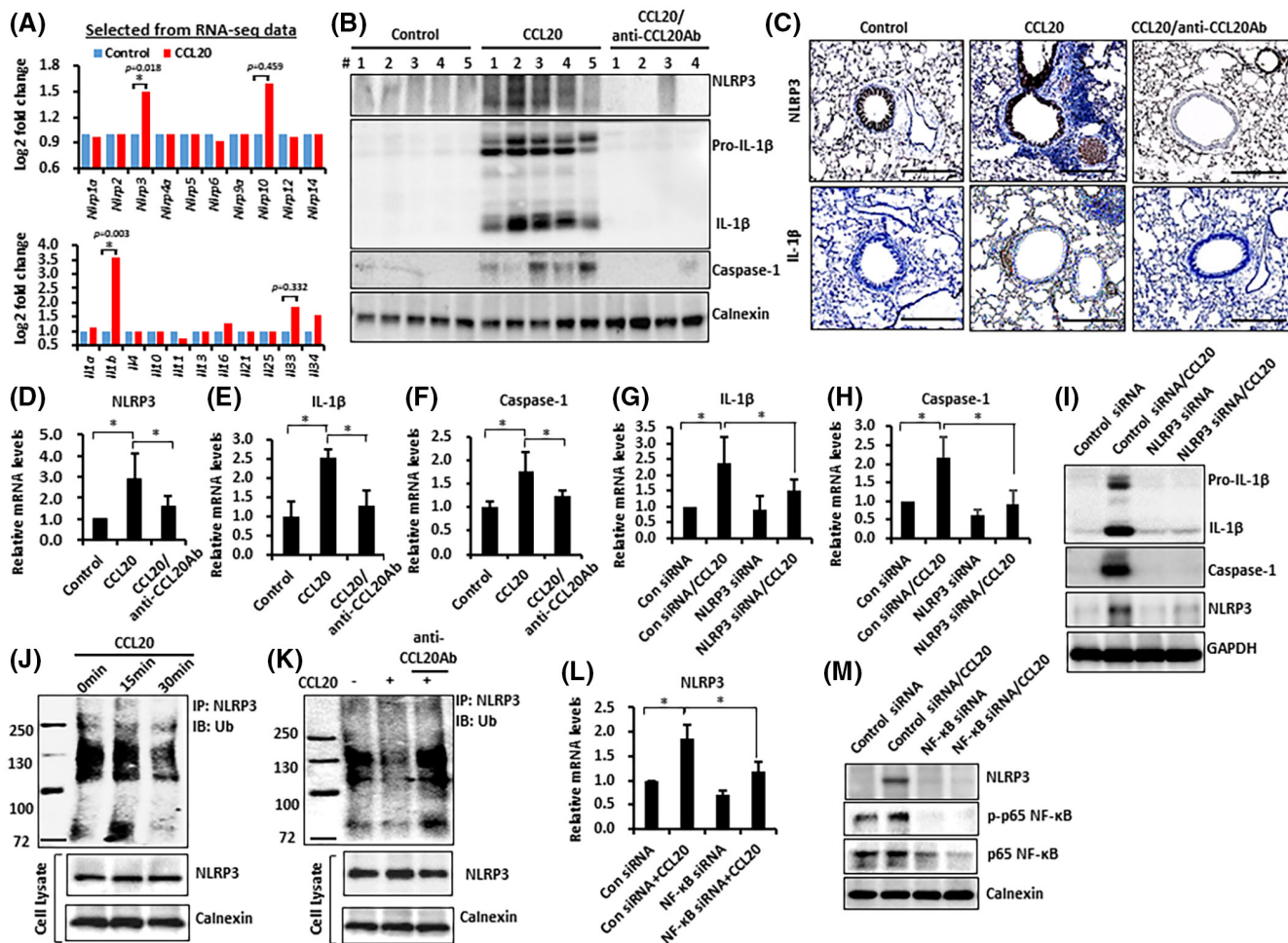


FIGURE 4 C-C chemokine ligand 20 (CCL20) is related to NLRP3 inflammasome activation in a mouse model of bronchial asthma. (A) Expressions of selected inflammatory response genes from RNA-seq data. Control ($n = 3$) and CCL20 ($n = 2$). $*p < .05$, two-sample t-test with unequal variance. (B) Lung protein lysates were analyzed using western blotting. (C) Tissue sections were stained using anti-IL-1 β and anti-Nod-like receptor family, pyrin domain-containing 3 (NLRP3). (D–F) BEAS-2B cells were treated with CCL20 (100 ng/ml) or co-treated with CCL20 (100 ng/ml) and anti-CCL20Ab (10 μ g/ml) for 2 h. The cells were harvested, and total RNA was isolated using TRIzol reagent. Transcripts were analyzed using reverse transcription-quantitative polymerase chain reaction (RT-qPCR). Data represent the mean \pm standard error of the mean (SEM) of three independent experiments. $*p < .05$; one-way analysis of variance (ANOVA). (G–I) The cells were transfected with 100 nM NLRP3 siRNA or control siRNA for 72 h and then treated with CCL20 (100 ng/ml) for (G and H) 2 h and (I) 6 h. mRNA and protein levels from lung lysates were analyzed using RT-qPCR and western blotting, respectively. Data represent the mean \pm SEM of three independent experiments. $*p < .05$; one-way ANOVA. (J) The cells were treated with CCL20 (100 ng/ml) for the indicated times. Proteins were immunoprecipitated with NLRP3 for 24 h and blotted with ubiquitin antibody. (K) The cells were treated with CCL20 (100 ng/ml) or co-treated with CCL20 (100 ng/ml) and anti-CCL20Ab (10 μ g/ml) for 30 min. Proteins were immunoprecipitated with NLRP3 for 24 h and blotted with anti-ubiquitin antibody. (L and M) The cells were transfected with 100 nM nuclear factor (NF)- κ B siRNA or control siRNA for 72 h and then treated with CCL20 (100 ng/ml) for (L) 2 h and (M) 6 h. Protein and mRNA levels were analyzed using RT-qPCR and western blotting, respectively. Data represent the mean \pm SEM of three independent experiments. $*p < .05$; one-way ANOVA.

in E-cadherin expression (Figure S2D–F). Therefore, we hypothesized that HDM-induced CCL20 might participate in EMT of airway remodeling. We analyzed the contribution of EMT to airway remodeling in chronic CCL20-treated mice and observed that vimentin expression was significantly increased in CCL20-treated mice compared to controls, while E-cadherin expression was significantly reduced (Figure 5A–C, $p < .05$). As expected, anti-CCL20Ab treatment rescued the expression levels of vimentin and

E-cadherin to those of the control (Figure 5A–C). We confirmed the effect of CCL20 on the expression of vimentin and E-cadherin in BEAS-2B cells. As shown in Figure 5D–F, CCL20 enhanced vimentin expression and reduced E-cadherin expression, whereas anti-CCL20Ab treatment ameliorated these effects. Immunofluorescence analysis also showed that CCL-20 treatment completely suppressed the expression of E-cadherin and anti-CCL20Ab reversed this effect (Figure 5G). These data indicate that

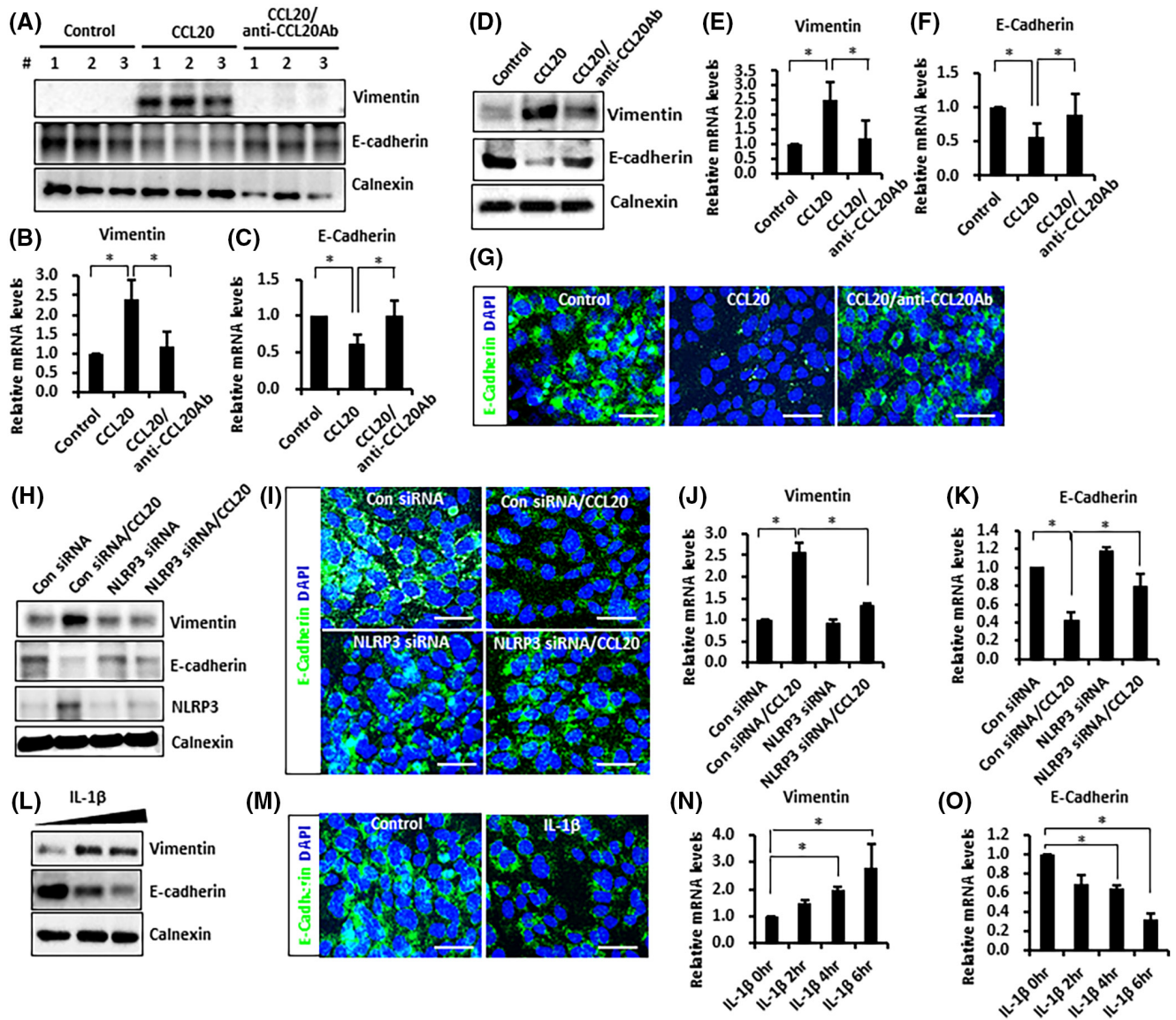


FIGURE 5 C-C chemokine ligand 20 (CCL20) participates in the regulation of epithelial-to-mesenchymal transition. (A) Lung protein lysates were analyzed by western blotting. (B and C) Lung mRNAs from the lungs of each mouse were analyzed with reverse transcription-quantitative polymerase chain reaction (RT-qPCR) using specific primer sets. Data represent the mean \pm standard error of the mean (SEM; $n = 5$ for each group). * $p < .05$; one-way analysis of variance (ANOVA). (D and F) BEAS-2B cells were treated with CCL20 (100 ng/ml) or co-treated with CCL20 (100 ng/ml) and anti-CCL20Ab (10 μ g/ml) for (D) 24 h and (E and F) 6 h. Protein and mRNA expression were analyzed using western blotting and RT-qPCR. Data represent the mean \pm SEM of three independent experiments. * $p < .05$; one-way ANOVA. (G) BEAS-2B cells were treated with CCL20 (100 ng/ml) or co-treated with CCL20 (100 ng/ml) and anti-CCL20 Ab (10 μ g/ml) for 24 h, and then the cells were stained with anti-E-cadherin (green). (H) The cells were transfected with 100 nM Nod-like receptor family, pyrin domain-containing 3 (NLRP3) siRNA or control siRNA for 72 h and then treated with CCL20 (100 ng/ml) for (H and I) 24 h and (J and K) 6 h. (H) Protein and (J and K) mRNA levels were analyzed using western blotting and RT-qPCR, respectively. Data represent the mean \pm SEM of three independent experiments. * $p < .05$; one-way ANOVA. (I) The cells were stained with anti-E-cadherin (green). (L) The cells were treated with IL-1 β (10 ng or 100 ng/ml) for 24 h. Proteins were harvested and analyzed using western blotting. (M) The cells were treated with IL-1 β (100 ng/ml) for 24 h, and then cells were stained with anti-E-cadherin. (N and O) The cells were treated with IL-1 β (100 ng/ml) for the indicated times. Total RNA was isolated using TRIzol reagent. mRNA levels were analyzed using RT-qPCR. Data represent the mean \pm SEM of three independent experiments. * $p < .05$; one-way ANOVA.

CCL20 leads to EMT in the lung epithelium. To further investigate whether the NLRP3 inflammasome is related to CCL20-mediated EMT, we transfected BEAS-2B cells with NLRP3

siRNA, the effect of CCL20 on vimentin upregulation and E-cadherin reduction were inhibited both at the protein (Figure 5H,I) and mRNA (Figure 5J,K) levels. These results suggest that the NLRP3 inflammasome is involved

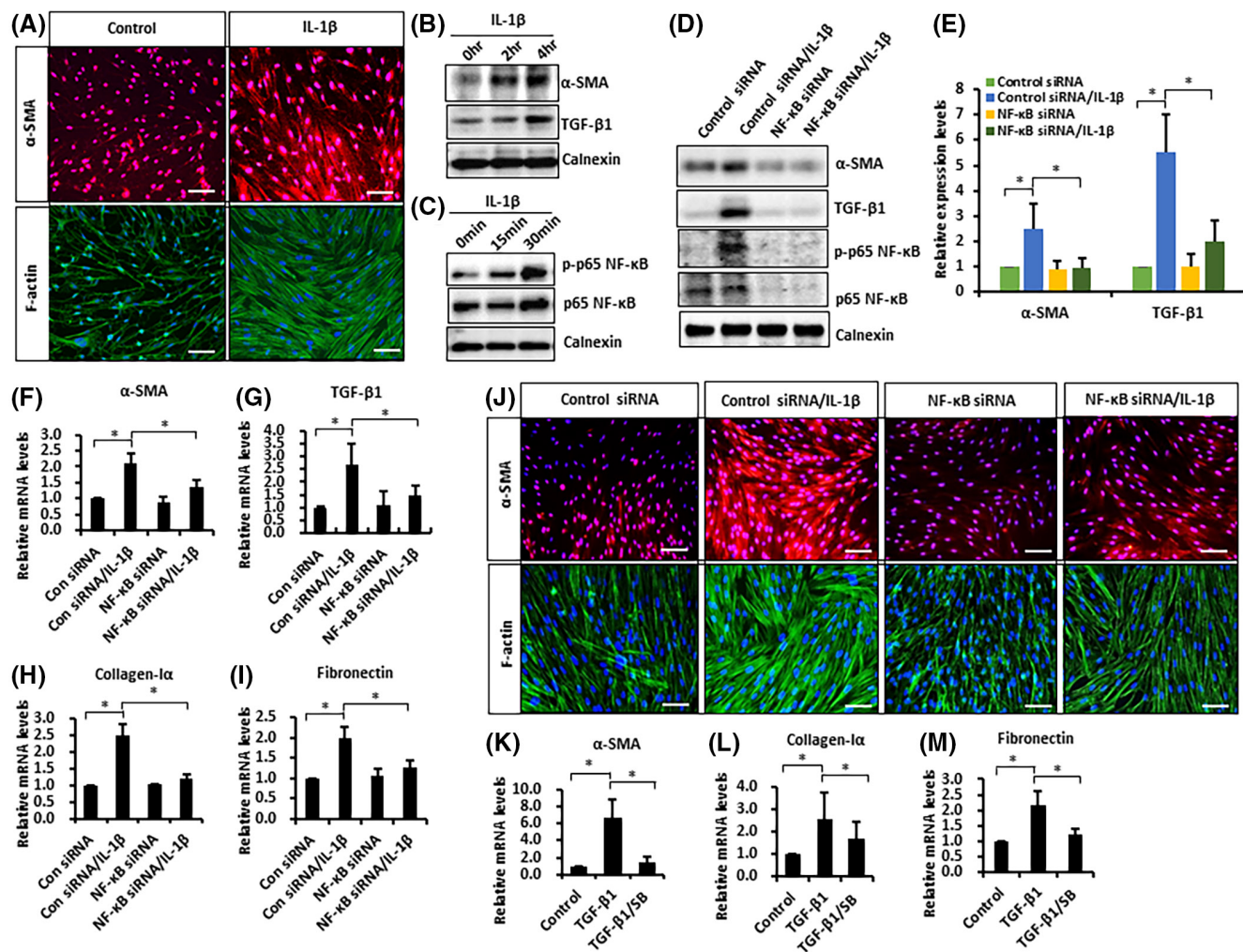


FIGURE 6 C-C chemokine ligand 20 (CCL20)-mediated IL-1 β is required for lung fibrosis in human lung fibroblasts. (A) IMR90 cells (human lung fibroblasts) were treated with interleukin (IL)-1 β (100 ng/ml) for 24 h. The cells were stained with anti-alpha-smooth muscle actin (α -SMA; red) and anti-F-actin (green). (B and C) The cells were treated with IL-1 β (100 ng/ml) for the indicated times. Protein levels were analyzed using western blotting. (D–I) The cells were transfected with 100 nM nuclear factor (NF)- κ B siRNA or control siRNA for 72 h and then stimulated with IL-1 β (100 ng/ml) for (D and E) 24 h and (F–I) 6 h. Protein and mRNA levels were analyzed using western blotting and reverse transcription-quantitative polymerase chain reaction (RT-qPCR), respectively. Data represent the mean \pm standard error of the mean (SEM) of three independent experiments. * p < .05; one-way analysis of variance (ANOVA). (J) The cells were transfected with 100 nM NF- κ B siRNA or control siRNA for 72 h and then stimulated with IL-1 β (100 ng/ml) for 24 h. The cells were stained with anti- α -SMA (red) and anti-F-actin (green). (K–M) The cells were pretreated with the transforming growth factor-beta 1 (TGF- β 1) inhibitor, SB431542, for 1 h and stimulated with TGF- β 1 (10 μ g/ml) for 6 h. mRNA levels were analyzed using RT-qPCR. Data represent the mean \pm SEM of three independent experiments. * p < .05; one-way ANOVA.

in CCL20-mediated EMT. IL-1 β promotes EMT by initiating crucial changes in protein expression.³⁷ To address whether any features of EMT were induced by IL-1 β , BEAS-2B cells were treated with different concentrations of IL-1 β . IL-1 β upregulated vimentin and downregulated E-cadherin expression in a concentration-dependent manner (Figure 5L). We also demonstrated the effect of IL-1 β on E-cadherin expression by immunofluorescence staining (Figure 5M). Furthermore, IL-1 β upregulated vimentin and downregulated E-cadherin in a time-dependent manner (Figure 5N,O). These results indicate that IL-1 β is involved in EMT in bronchial epithelial cells, and that

CCL20/NLRP3-mediated secretion of IL-1 β plays an important role in EMT leading to lung fibrosis.

3.6 | CCL20/NLRP3-mediated secretion of IL-1 β promotes myfibroblast recruitment through the TGF- β 1/ α -SMA/Collagen-1 α profibrotic pathway in human lung fibroblasts

In IMR90, human lung fibroblasts, immunofluorescence staining revealed that IL-1 β promoted α -SMA expression

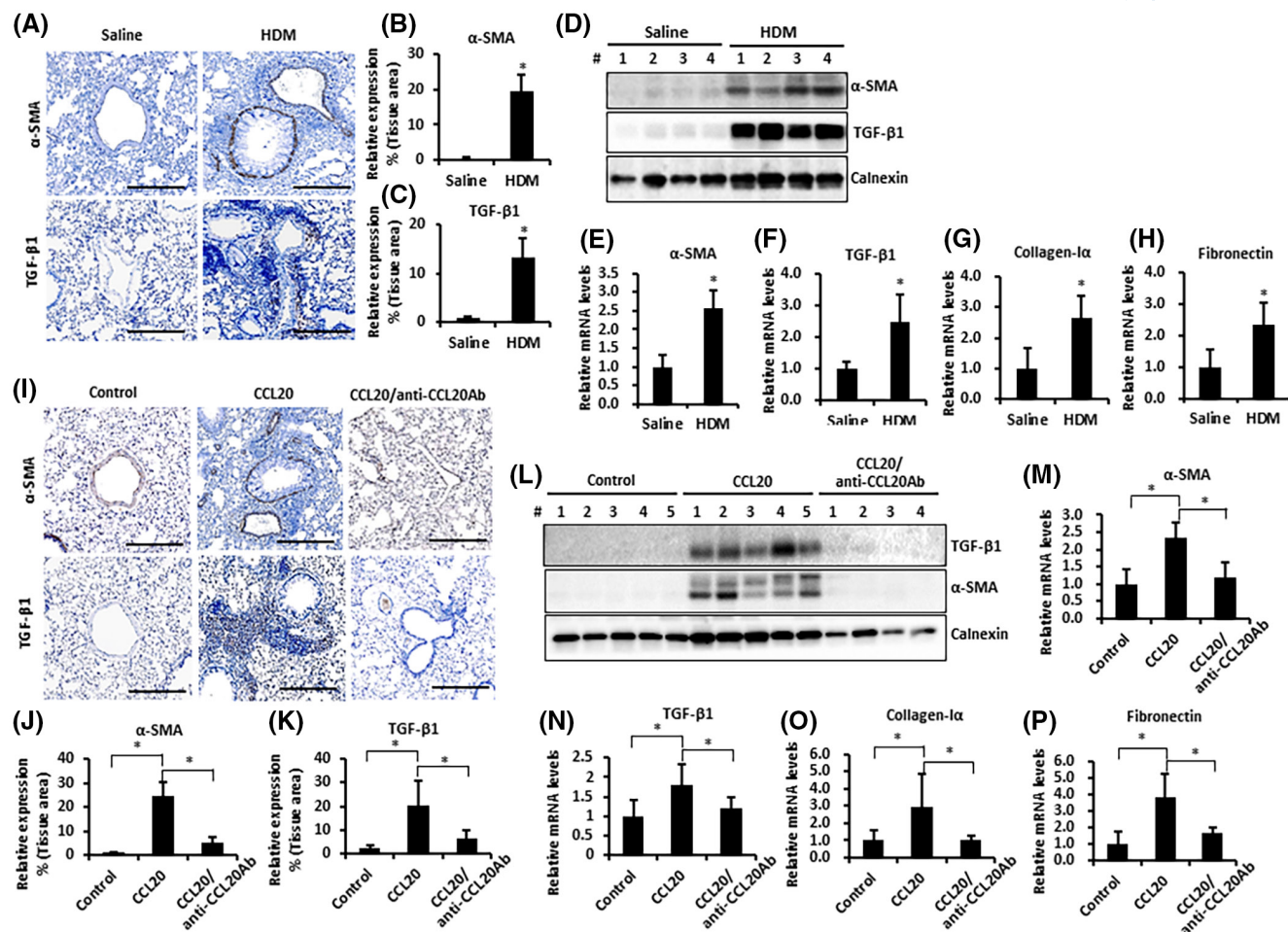
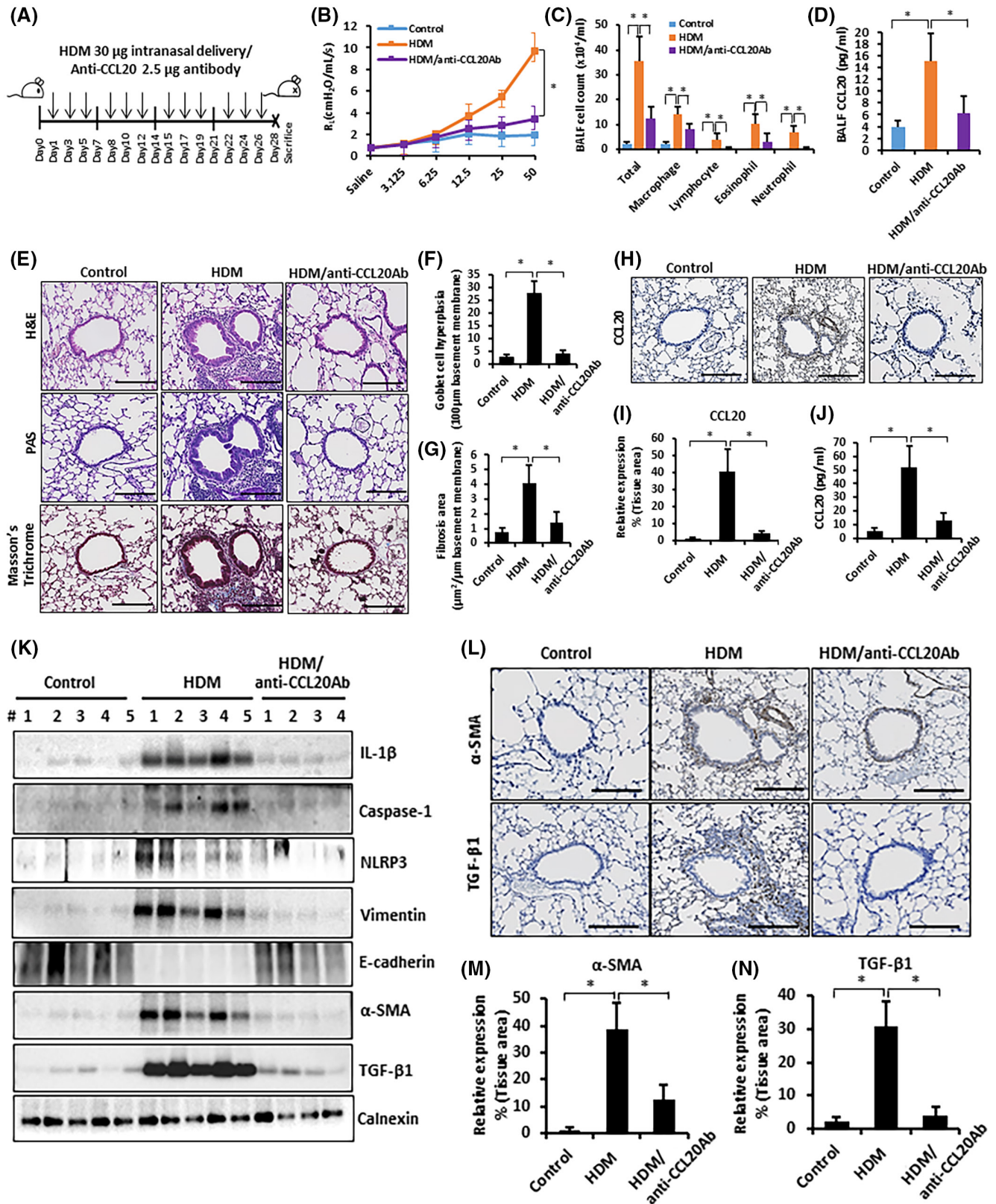


FIGURE 7 House dust mite (HDM)-induced C-C chemokine ligand 20 (CCL20) is required for lung fibrosis in a mouse model of bronchial asthma. (A) Tissue sections were stained using anti-alpha-smooth muscle actin (α -SMA) or anti-transforming growth factor-beta 1 (TGF- β 1). (B and C) Quantitative analyses of immunostaining area for peribronchial α -SMA and TGF- β 1 were analyzed using Zeiss Cell Observer. Data represent the mean \pm standard error of the mean (SEM; $n = 5$ for each group). $*p < .05$; Student t test. (D) Lung protein lysates were analyzed using western blotting. (E–H) Lung mRNAs were analyzed with reverse transcription-quantitative polymerase chain reaction (RT-qPCR). Data represent the mean \pm SEM ($n = 5$ for each group). $*p < .05$; Student t test. (I) Tissue sections were stained using anti- α -SMA or anti-TGF- β 1. (J and K) Quantitative analyses of the immunostaining area for peribronchial α -SMA and TGF- β 1 were analyzed using Zeiss Cell Observer. Data represent the mean \pm SEM ($n = 5$ for each group). $*p < .05$; one-way analysis of variance (ANOVA). (L) Lung protein lysates were analyzed by western blotting. (M–P) Lung mRNAs were analyzed with RT-qPCR. Data represent the mean \pm SEM ($n = 5$ for each group). $*p < .05$; one-way ANOVA.

and F-actin cytoskeleton reorganization which is a key indicator of lung fibrosis (Figure 6A). As shown in Figure 6B, IL-1 β upregulated α -SMA expression and TGF- β 1 expression. TGF- β 1 is an important profibrotic cytokine that targets epithelial cells, and induces EMT and ECM-producing myofibroblast formation. Next, we examined the role of NF- κ B in the regulation of IL-1 β -mediated profibrotic factors such as TGF- β 1, α -SMA, and collagen I in IMR90 cells, because NF- κ B is a transcription factor that mediates expression of profibrotic factors. We observed that IL-1 β induced NF- κ B activation (Figure 6C), and in cells transfected with NF- κ B siRNA, IL-1 β -induced TGF- β 1 and α -SMA expression

was decreased compared to IL-1 β -treated control siRNA-transfected cells (Figure 6D,E). Additionally, IL-1 β -induced TGF- β 1, α -SMA, collagen-1 α , and fibronectin mRNA expression was suppressed by NF- κ B siRNA, compared to IL-1 β -treated control siRNA-transfected cells (Figure 6F–I). Furthermore, NF- κ B knockdown inhibited α -SMA and F-actin cytoskeleton reorganization (Figure 6J).

Next, we confirmed the effect of TGF- β 1 on myofibroblast differentiation of IMR90 cells. TGF- β 1 contributes to smooth muscle hyperplasia by promoting fibroblast differentiation into myofibroblasts. TGF- β 1 induced α -SMA and F-actin cytoskeleton reorganization (Figure S3). However,



α -SMA, collagen-1 α , and fibronectin mRNA expressions were decreased by SB431542, a TGF- β inhibitor (Figure 6K–M). Taken together, our results show that IL-1 β acts as a

major player in profibrotic processes through the TGF- β 1/ α -SMA/collagen-1 α profibrotic pathway, leading to the differentiation of human lung fibroblasts into myofibroblasts.

FIGURE 8 Anti-C-C chemokine ligand 20 (CCL20) restores house dust mite (HDM)-induced airway hyper-responsiveness (AHR) and airway remodeling in a mouse model of bronchial asthma. (A) Schedule for preparation of the allergic airway disease model. Eight-week-old BALB/c mice were intranasally administered HDM (30 µg) or co-treated with HDM (30 µg) and anti-CCL20Ab (2.5 µg) for 3 days/week for 4 weeks. Sacrifice was performed on the 28th day. (B) AHR was measured using airway resistance and compliance to metacholine. Data represent the mean ± standard error of the mean (SEM; $n = 5$ for each group). * $p < .05$; one-way analysis of variance (ANOVA). (C) Immune cells in BAL fluid were counted. Data represent the mean ± SEM ($n = 5$ for each group). * $p < .05$; one-way ANOVA. (D) CCL20 levels in BAL fluid were measured by ELISA. Data represent the mean ± SEM ($n = 5$ for each group). * $p < .05$; one-way ANOVA. (E) Tissue sections were stained using hematoxylin and eosin (H&E), periodic acid-Schiff (PAS) and Masson's Trichrome. The number of goblet cells (F) and the fibrotic area (G) were analyzed using Zeiss Cell Observer. Data are expressed as the mean ± SEM ($n = 5$ for each group). * $p < .05$; one-way ANOVA. (H) Tissue sections were stained using anti-CCL20. (I) Quantitative analyses of immunostaining area for bronchial CCL20 were analyzed using Zeiss Cell Observer. Data represent the mean ± SEM ($n = 5$ for each group). * $p < .05$; one-way ANOVA. (J) CCL20 was measured in lung homogenates by ELISA. Data represent the mean ± SEM ($n = 5$ for each group). * $p < .05$; one-way ANOVA. (K) Expression of protein isolated from lung lysates was analyzed by western blotting, respectively. (L) Tissue sections were stained using anti- α -SMA or anti-TGF- β 1. (M and N) Quantitative analyses of immunostaining area for peribronchial α -SMA and TGF- β 1 were analyzed using Zeiss Cell Observer. Data represent the mean ± SEM ($n = 5$ for each group). * $p < .05$; one-way ANOVA.

3.7 | Anti-CCL20 attenuates airway remodeling in a HDM-induced bronchial asthma mouse model

Increased airway smooth muscle mass and fibroblast dysfunction result in airway remodeling.³⁸ Histologic examination revealed that HDM-induced α -SMA and TGF- β 1 were enhanced in the peribronchiolar areas (Figure 7A–C). We also showed that HDM increased α -SMA, TGF- β 1, collagen-I α , and fibronectin levels in mouse models (Figure 7D–H). We further observed that CCL20-induced α -SMA and TGF- β 1 expression was decreased in the peribronchiolar areas following anti-CCL20Ab treatment (Figure 7I–K). Additionally, CCL20-induced α -SMA, TGF- β 1, collagen-I α , and fibronectin protein and gene expression was suppressed by anti-CCL20Ab treatment of mouse models (Figure 7L–P). These results demonstrate that anti-CCL20Ab attenuates lung fibrosis in a CCL20-mediated mouse model of bronchial asthma.

To evaluate the effect of anti-CCL20Ab on the HDM-mediated bronchial airway remodeling, we employed a mouse model of HDM-induced airway inflammation. In this experiment, saline (control), 30 µg HDM, or 30 µg HDM with 2.5 µg of anti-CCL20Ab was intranasally administered (Figure 8A). Airway resistance to MeCh was measured using a flexiVent system after the mice were anesthetized on day 28. HDM-induced AHR to MeCh was markedly inhibited by anti-CCL20Ab compared to HDM-treated mice ($p < .05$) (Figure 8B). In addition, the number of inflammatory cells in BALF was significantly decreased in the anti-CCL20Ab co-treated mice compared to HDM-treated mice (Figure 8C), suggesting that anti-CCL20Ab strongly inhibits allergic inflammation. We also detected the decreased levels of CCL20 in the anti-CCL20Ab co-treated mice compared to HDM-treated mice in BALF (Figure 8D). Histological analysis (H&E staining) of lung tissue demonstrated a marked reduction

in the inflammatory cells around the airway in anti-CCL20Ab co-treated mice compared to the HDM-treated mice (Figure 8E). Moreover, PAS staining showed that goblet cells containing mucus were markedly decreased in the anti-CCL20Ab co-treated mice compared to HDM-treated mice (Figure 8E,F). Masson's trichrome staining revealed that anti-CCL20Ab reduced subepithelial fibrosis surrounding the airways of lung tissues (Figure 8E,G), suggesting that anti-CCL20Ab mediates HDM-induced bronchial airway remodeling. We also found that HDM-induced CCL20 levels were decreased by anti-CCL20Ab in histological analysis of CCL20 staining (Figure 8H,I) and protein samples of lung tissue (Figure 8J). As shown in Figure 8K, the expression level of IL-1 β , Caspase-1 or NLRP3 induced by HDM was decreased in anti-CCL20Ab co-treated mice, indicating a critical role of CCL20 in NLRP3 inflammasome activation in HDM-induced airway inflammation. In addition, we observed that the increased expression of vimentin and the decreased expression of E-cadherin by HDM were restored by treatment with anti-CCL20Ab. Moreover, HDM-induced α -SMA and TGF- β 1 expression was suppressed by anti-CCL20Ab treatment. Furthermore, histologic examination revealed that HDM-induced α -SMA and TGF- β 1 were inhibited in the anti-CCL20Ab co-treated mice compared to HDM-treated mice (Figure 8L–N). Taken together, these results demonstrate that anti-CCL20Ab attenuates airway inflammation and remodeling in a HDM-induced bronchial asthma mouse model.

4 | DISCUSSION

In this study, we found that CCL20 production is regulated by the HDM-mediated Akt-ERK1/2-C/EBP β pathway and that CCL20 regulates chronic airway inflammation by increasing activation of the NLRP3 inflammasome through

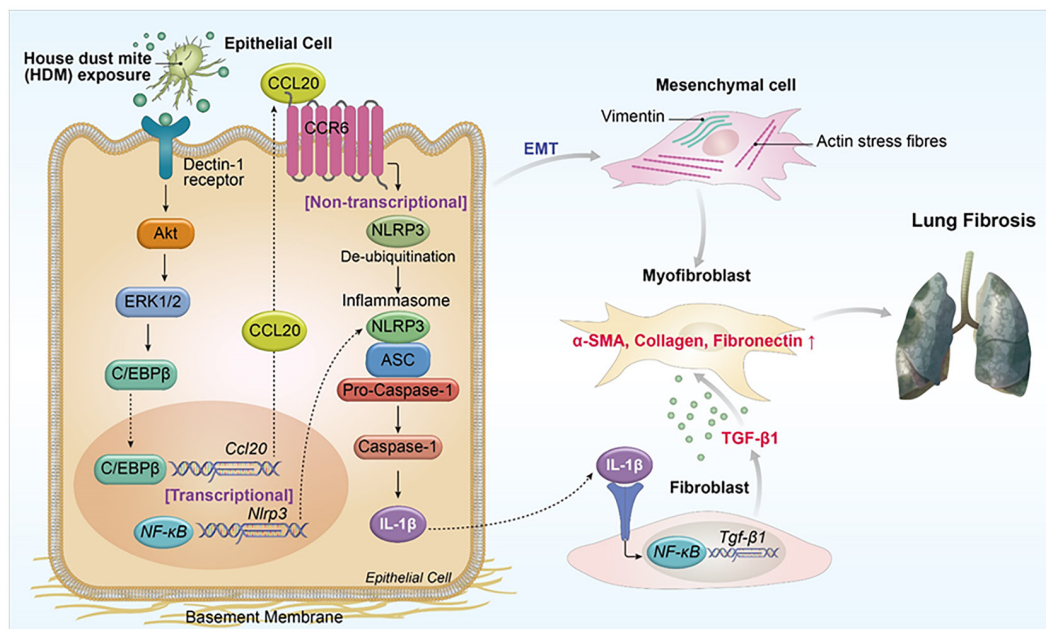


FIGURE 9 Proposed model of house dust mite (HDM)-induced C–C chemokine ligand 20 (CCL20) production in chronic airway inflammation and remodeling. HDM-induced CCL20 is regulated by the Akt-ERK1/2-C/EBP β pathway, which enhances Nod-like receptor family, pyrin domain-containing 3 (NLRP3) inflammasome activation. Furthermore, we demonstrated that CCL20-mediated NLRP3 activation is required for chronic inflammation response, subepithelial fibrosis for airway remodeling in allergic asthma.

two processes: NLRP3 ubiquitination and transcriptional upregulation. Moreover, HDM-induced CCL20 is required for EMT production through regulation profibrotic factors. Anti-CCL20Ab administration attenuated NLRP3 inflammasome activation and EMT-mediated airway remodeling in HDM asthma model. The findings of the present study are summarized in [Figure 9](#).

Allergic asthma is a chronic inflammatory airway disease characterized by increased bronchial mucosa, goblet cell hyperplasia, and dysfunctional airway constitutional cells.³⁹ Thus, chronic airway inflammation can be described as the major force driving the processes leading to most aspects of airway remodeling.³⁸ Previous studies have shown that HDM exposure is associated with epithelial damage and airway remodeling during the development of chronic asthma. In the present study, we also showed that HDM treatment causes allergic airway inflammation in an animal model of asthma. Furthermore, HDM-induced CCL20 triggered thickening of the airway, including inflammatory cell infiltration into the peribronchial space around the airway and increased goblet cell numbers. However, HDM or CCL20-induced allergic airway inflammation and remodeling were remarkably suppressed by treatment with anti-CCL20Ab in the animal model. Differentiation of airway epithelial cells into goblet cells is directed by other structural cells in the submucosa.⁴⁰ Importantly, it is reported that anti-CCL20 treatment significantly decreased virus-induced mucus production.⁴¹ The cross-talk between the epithelial layer

and airway smooth muscle cells (ASMC) might be significant to understanding the progression of airway remodeling. Therefore, it appears to be elucidated the cross-talk between ASMCs and epithelial cells on HDM-mediated CCL20 activation in inflammatory airway remodeling in the future study.

Inflammasomes are the most studied innate immune response mechanisms against infection. These complexes are expressed in various immune cells, including macrophages, neutrophils, T cells, epithelial cells, and myofibroblasts.⁴² The critical action of the inflammasome is caspase-1 activation, which leads to IL-1 β cleavage and secretion.⁴³ IL-1 β -deficient (IL-1 $\beta^{-/-}$) mice show reduced neutrophilic inflammation and ameliorated asthma.⁴⁴ In this study, we showed increased caspase-1 and IL-1 β levels in a CCL20-induced asthma mouse model. Caspase-1 and IL-1 β levels decreased following treatment of the asthma mouse model with an anti-CCL20Ab. Therefore, we hypothesized that CCL20 is involved in inflammasome activation. We screened for inflammasome subtypes using RNA-seq analysis and confirmed the inflammasome expression. NLRP activity mainly occurs in macrophages and neutrophils. Interestingly, we found that the numbers of macrophages and neutrophils was significantly increased in the CCL-20-induced asthma mouse model. Furthermore, we observed that CCL20 regulates NLRP3 activity by promoting NLRP3 deubiquitination and NLRP3 expression via NF- κ B transcriptional regulation. These results demonstrate that CCL20 is required for NLRP3

inflammasome activation, subsequently leading to IL-1 β production, which is critical for the induction of allergic airway inflammation. Recent studies have shown that NLRP3 inflammasome activity is also closely related to TLRs.⁴⁵ In addition, HDM-derived β -glucan acts through Toll-like receptor 2 (TLR2) to induce immune responses.⁴⁶ Moreover, HDM-induced airway inflammation is LPS/TLR4 dependent,⁴⁷ indicating that HDM-induced allergic airway inflammation is related to various mechanisms, especially TLRs. Although this study focused on the role of CCL20-mediated NLRP3 activation through HDM/dectin-1 receptor signaling in airway inflammation, it is possible that the present study may be relevant to at least some part of the TLR-mediated inflammatory response.

EMT is a crucial process in airway remodeling and lung fibrosis in asthma. Currently, most studies of CCL20 in EMT report that CCL20 is related to cancer cell migration,^{48,49} but their role in lung fibrosis has not been identified yet. In the present study, HDM extract or CCL20 decreased E-cadherin expression and increased vimentin expression in bronchial epithelial cells and mouse models. In contrast, anti-CCL20Ab treatment showed remarkable effects on EMT progression, suggesting that CCL20 is involved in EMT modulation. In addition, NLRP3 knockdown inhibited EMT in bronchial epithelial cells treated with CCL20. These results demonstrate that CCL20-mediated NLRP3 activation is closely linked to EMT in airway remodeling and lung fibrosis. Recent studies have shown that myofibroblasts are a key cellular factor in lung fibrosis and serve as collagen-producing cells when activated.⁵⁰ Collagen secretion is increased, which promotes the deposition of extracellular matrix proteins such as fibronectin, and leads to the development of lung fibrosis.⁵¹ Consistently, we observed increased α -SMA, TGF- β 1, collagen-1, and fibronectin levels in HDM extract or CCL20-treated bronchial epithelial cells and mouse models.

Here, we demonstrate a novel mechanism for HDM-induced CCL20 expression and secretion through the Akt-ERK1/2-C/EBP β pathway, which promotes NLRP3 inflammasome activity and EMT progression. In addition, IL-1 β activates TGF- β 1 by NF- κ B transcriptional regulation and promotes myofibroblast differentiation in lung fibroblasts. We therefore propose that these findings provide insight into HDM-mediated CCL20 function in airway inflammation and a potential contribution to airway remodeling in allergic asthma. Recent study suggests that interfering with chemokines or chemokine receptors represents a new approach in allergy therapy.⁵² Therefore, this study will provide a new approach to the treatment of allergic asthma through chemokine regulation by elucidating the HDM-induced CCL20 expression and its effect on airway remodeling.

AUTHOR CONTRIBUTIONS

Shin-Young Park performed and analyzed most of the experiments, original draft preparation and provided the requested funding. Min-Jeong Kang and Nuri Jin helped mouse experiments. So Young Lee, Yun Young Lee and Sungsin Jo helped cell experiments. Jeong Yun Eom helped IHC. Heejae Han and Sook In Chung analyzed mouse data. Kiseok Jang, Tae-Hwan Kim and Jungwon Park participated in experimental design and interpretation of data. Joong-Soo Han supervised the project. All authors approved the final version of the manuscript.

ACKNOWLEDGMENTS

This work was supported by the National Research Foundation of Korea (NRF) grant funded by the Korea government (MSIT) (2021R1A2C1008317), and partly supported by the National Research Foundation of Korea (NRF), which is funded by the Ministry of Science, ICT, and Future Planning (2018R1A1A1A05022185). We also thank Prof. Eung-Gook Kim (Chungbuk University, Republic of Korea) for providing IMR90 cells in this study.

DISCLOSURES

The authors declare that they have no conflict of interest.

DATA AVAILABILITY STATEMENT

The data that support the findings of this study are available on request from the corresponding author.

ORCID

Shin-Young Park  <https://orcid.org/0000-0002-6073-4634>

Joong-Soo Han  <https://orcid.org/0000-0002-0875-6158>

REFERENCES

- Huang FL, Liao EC, Yu SJ. House dust mite allergy: its innate immune response and immunotherapy. *Immunobiology*. 2018;223:300-302.
- Porsbjerg C, Baines K, Gibson P, et al. IL-33 is related to innate immune activation and sensitization to HDM in mild steroid-free asthma. *Clin Exp Allergy*. 2016;46:564-574.
- Hong GH, Kwon HS, Moon KA, et al. Clusterin modulates allergic airway inflammation by attenuating CCL20-mediated dendritic cell recruitment. *J Immunol*. 2016;196:2021-2030.
- Nathan AT, Peterson EA, Chakir J, Wills-Karp M. Innate immune responses of airway epithelium to house dust mite are mediated through beta-glucan-dependent pathways. *J Allergy Clin Immunol*. 2009;123:612-618.
- Schutysse E, Struyf S, Van Damme J. The CC chemokine CCL20 and its receptor CCR6. *Cytokine Growth Factor Rev*. 2003;14:409-426.
- Lee AY, Korner H. CCR6 and CCL20: emerging players in the pathogenesis of rheumatoid arthritis. *Immunol Cell Biol*. 2014;92:354-358.
- Pichavant M, Charbonnier AS, Taront S, et al. Asthmatic bronchial epithelium activated by the proteolytic allergen Der p 1

- increases selective dendritic cell recruitment. *J Allergy Clin Immunol.* 2005;115:771-778.
8. Weckmann M, Collison A, Simpson JL, et al. Critical link between TRAIL and CCL20 for the activation of TH2 cells and the expression of allergic airway disease. *Nat Med.* 2007;13:1308-1315.
 9. Artlett CM. The role of the NLRP3 inflammasome in fibrosis. *Open Rheumatol J.* 2012;6:80-86.
 10. Gasse P, Mary C, Guenon I, et al. IL-1R1/MyD88 signaling and the inflammasome are essential in pulmonary inflammation and fibrosis in mice. *J Clin Invest.* 2007;117:3786-3799.
 11. Juliana C, Fernandes-Alnemri T, Kang S, Farias A, Qin F, Alnemri ES. Non-transcriptional priming and deubiquitination regulate NLRP3 inflammasome activation. *J Biol Chem.* 2012;287:36617-36622.
 12. Franchi L, Munoz-Planillo R, Nunez G. Sensing and reacting to microbes through the inflammasomes. *Nat Immunol.* 2012;13:325-332.
 13. Zahid A, Li B, Kombe AJK, Jin T, Tao J. Pharmacological inhibitors of the NLRP3 inflammasome. *Front Immunol.* 2019;10:2538.
 14. Gros Lambert M, Py BF. Spotlight on the NLRP3 inflammasome pathway. *J Inflamm Res.* 2018;11:359-374.
 15. Broz P, Dixit VM. Inflammasomes: mechanism of assembly, regulation and signalling. *Nat Rev Immunol.* 2016;16:407-420.
 16. Song C, He L, Zhang J, et al. Fluorofenidone attenuates pulmonary inflammation and fibrosis via inhibiting the activation of NALP3 inflammasome and IL-1beta/IL-1R1/MyD88/NF-kappaB pathway. *J Cell Mol Med.* 2016;20:2064-2077.
 17. Hirata T, Osuga Y, Takamura M, et al. Recruitment of CCR6-expressing Th17 cells by CCL20 secreted from IL-1 beta-, TNF-alpha-, and IL-17A-stimulated endometriotic stromal cells. *Endocrinology.* 2010;151:5468-5476.
 18. Hosokawa Y, Hosokawa I, Shindo S, Ozaki K, Matsuo T. IL-4 modulates CCL11 and CCL20 productions from IL-1beta-stimulated human periodontal ligament cells. *Cell Physiol Biochem.* 2016;38:153-159.
 19. Lu A, Li H, Niu J, et al. Hyperactivation of the NLRP3 inflammasome in myeloid cells leads to severe organ damage in experimental lupus. *J Immunol.* 2017;198:1119-1129.
 20. Nieto MA, Huang RY, Jackson RA, Thiery JP. EMT: 2016. *Cell.* 2016;166:21-45.
 21. Hill C, Jones MG, Davies DE, Wang Y. Epithelial-mesenchymal transition contributes to pulmonary fibrosis via aberrant epithelial/fibroblastic cross-talk. *J Lung Health Dis.* 2019;3:31-35.
 22. Xiao Fenglin WS, Zhang Zhiyong Y, Hai LM. Pirfenidone ameliorated AGE-induced EMT and attenuated peritoneal fibrosis in peritoneal mesothelial cells. *Mol Cell Toxicol.* 2021;17:315-323.
 23. Halwani R, Al-Muhsen S, Al-Jahdali H, Hamid Q. Role of transforming growth factor-beta in airway remodeling in asthma. *Am J Respir Cell Mol Biol.* 2011;44:127-133.
 24. Jacquet A. Innate immune responses in house dust mite allergy. *ISRN Allergy.* 2013;2013:735031.
 25. Lee HM, Yuk JM, Shin DM, Jo EK. Dectin-1 is inducible and plays an essential role for mycobacteria-induced innate immune responses in airway epithelial cells. *J Clin Immunol.* 2009;29:795-805.
 26. Sperling T, Oldak M, Walch-Ruckheim B, et al. Human papillomavirus type 8 interferes with a novel C/EBPbeta-mediated mechanism of keratinocyte CCL20 chemokine expression and Langerhans cell migration. *PLoS Pathog.* 2012;8:e1002833.
 27. Mantena SR, Kannan A, Cheon YP, et al. C/EBPbeta is a critical mediator of steroid hormone-regulated cell proliferation and differentiation in the uterine epithelium and stroma. *Proc Natl Acad Sci U S A.* 2006;103:1870-1875.
 28. Shen F, Hu Z, Goswami J, Gaffen SL. Identification of common transcriptional regulatory elements in interleukin-17 target genes. *J Biol Chem.* 2006;281:24138-24148.
 29. Hu J, Roy SK, Shapiro PS, et al. ERK1 and ERK2 activate CCAAAT/enhancer-binding protein-beta-dependent gene transcription in response to interferon-gamma. *J Biol Chem.* 2001;276:287-297.
 30. Besnard AG, Guillou N, Tschopp J, et al. NLRP3 inflammasome is required in murine asthma in the absence of aluminum adjuvant. *Allergy.* 2011;66:1047-1057.
 31. Hirota JA, Hirota SA, Warner SM, et al. The airway epithelium nucleotide-binding domain and leucine-rich repeat protein 3 inflammasome is activated by urban particulate matter. *J Allergy Clin Immunol.* 2012;129:1116-1125.e6.
 32. Liu D, Yang P, Gao M, et al. NLRP3 activation induced by neutrophil extracellular traps sustains inflammatory response in the diabetic wound. *Clin Sci (Lond).* 2019;133:565-582.
 33. Shimizu H, Sakimoto T, Yamagami S. Pro-inflammatory role of NLRP3 inflammasome in experimental sterile corneal inflammation. *Sci Rep.* 2019;9:9596.
 34. Goto Y, Uchida Y, Nomura A, et al. Dislocation of E-cadherin in the airway epithelium during an antigen-induced asthmatic response. *Am J Respir Cell Mol Biol.* 2000;23:712-718.
 35. Holgate ST, Roberts G, Arshad HS, Howarth PH, Davies DE. The role of the airway epithelium and its interaction with environmental factors in asthma pathogenesis. *Proc Am Thorac Soc.* 2009;6:655-659.
 36. Heijink IH, Postma DS, Noordhoek JA, Broekema M, Kapus A. House dust mite-promoted epithelial-to-mesenchymal transition in human bronchial epithelium. *Am J Respir Cell Mol Biol.* 2010;42:69-79.
 37. Al-Alawi M, Hassan T, Chotirmall SH. Transforming growth factor beta and severe asthma: a perfect storm. *Respir Med.* 2014;108:1409-1423.
 38. Fehrenbach H, Wagner C, Wegmann M. Airway remodeling in asthma: what really matters. *Cell Tissue Res.* 2017;367:551-569.
 39. Proud D, Leigh R. Epithelial cells and airway diseases. *Immunol Rev.* 2011;242:186-204.
 40. Faiz A, Weckmann M, Tasena H, et al. Profiling of healthy and asthmatic airway smooth muscle cells following interleukin-1beta treatment: a novel role for CCL20 in chronic mucus hypersecretion. *Eur Respir J.* 2018;52:1800310.
 41. Kallal LE, Schaller MA, Lindell DM, Lira SA, Lukacs NW. CCL20/CCR6 blockade enhances immunity to RSV by impairing recruitment of DC. *Eur J Immunol.* 2010;40:1042-1052.
 42. Artlett CM, Thacker JD. Molecular activation of the NLRP3 Inflammasome in fibrosis: common threads linking divergent fibrogenic diseases. *Antioxid Redox Signal.* 2015;22:1162-1175.
 43. Dostert C, Petrilli V, Van Bruggen R, Steele C, Mossman BT, Tschopp J. Innate immune activation through Nalp3 inflammasome sensing of asbestos and silica. *Science.* 2008;320:674-677.
 44. Mahmutovic Persson I, Menzel M, Ramu S, Cerps S, Akbarshahi H, Uller L. IL-1beta mediates lung neutrophilia and IL-33

- expression in a mouse model of viral-induced asthma exacerbation. *Respir Res.* 2018;19:16.
45. Kelley N, Jeltema D, Duan Y, He Y. The NLRP3 inflammasome: an overview of mechanisms of activation and regulation. *Int J Mol Sci.* 2019;20:3328.
 46. Ryu JH, Yoo JY, Kim MJ, et al. Distinct TLR-mediated pathways regulate house dust mite-induced allergic disease in the upper and lower airways. *J Allergy Clin Immunol.* 2013;131:549-561.
 47. Hammad H, Chieppa M, Perros F, Willart MA, Germain RN, Lambrecht BN. House dust mite allergen induces asthma via Toll-like receptor 4 triggering of airway structural cells. *Nat Med.* 2009;15:410-416.
 48. Liu Y, Wang J, Ni T, Wang L, Wang Y, Sun X. CCL20 mediates RANK/RANKL-induced epithelial-mesenchymal transition in endometrial cancer cells. *Oncotarget.* 2016;7:25328-25339.
 49. Marsigliante S, Vetrugno C, Muscella A. Paracrine CCL20 loop induces epithelial-mesenchymal transition in breast epithelial cells. *Mol Carcinog.* 2016;55:1175-1186.
 50. Huang Q, Chen Y, Shen S, et al. Klotho antagonizes pulmonary fibrosis through suppressing pulmonary fibroblasts activation, migration, and extracellular matrix production: a therapeutic implication for idiopathic pulmonary fibrosis. *Aging (Albany NY).* 2020;12:5812-5831.
 51. Wang H, Lyu J, Chen L, Yu W. IL-17A activates mouse lung fibroblasts through promoting chemokine CXCL12 secretion. *Zhejiang Da Xue Bao Yi Xue Ban.* 2020;49:758-764.
 52. Garcia G, Godot V, Humbert M. New chemokine targets for asthma therapy. *Curr Allergy Asthma Rep.* 2005;5:155-160.

SUPPORTING INFORMATION

Additional supporting information can be found online in the Supporting Information section at the end of this article.

How to cite this article: Park S-Y, Kang M-J, Jin N, et al. House dust mite-induced Akt-ERK1/2-C/EBP beta pathway triggers CCL20-mediated inflammation and epithelial-mesenchymal transition for airway remodeling. *The FASEB Journal.* 2022;36:e22452. doi:[10.1096/fj.20220150RR](https://doi.org/10.1096/fj.20220150RR)